



**HAL**  
open science

## **Biomass prediction in tropical forests: the canopy grain approach**

Christophe Proisy, Nicolas Barbier, Michael Guérout, Raphaël Pélissier, Jean-Philippe Gastellu-Etchegorry, Eloi Grau, Pierre Couteron

### ► **To cite this version:**

Christophe Proisy, Nicolas Barbier, Michael Guérout, Raphaël Pélissier, Jean-Philippe Gastellu-Etchegorry, et al.. Biomass prediction in tropical forests: the canopy grain approach. Remote sensing of biomass: principles and applications, Intech, pp.1-18, 2011. ird-00658600

**HAL Id: ird-00658600**

**<https://ird.hal.science/ird-00658600>**

Submitted on 11 Jan 2012

**HAL** is a multi-disciplinary open access archive for the deposit and dissemination of scientific research documents, whether they are published or not. The documents may come from teaching and research institutions in France or abroad, or from public or private research centers.

L'archive ouverte pluridisciplinaire **HAL**, est destinée au dépôt et à la diffusion de documents scientifiques de niveau recherche, publiés ou non, émanant des établissements d'enseignement et de recherche français ou étrangers, des laboratoires publics ou privés.

# Biomass Prediction in Tropical Forests: The Canopy Grain Approach

Christophe Proisy<sup>1</sup>, Nicolas Barbier<sup>1</sup>, Michael Guérault<sup>2</sup>, Raphael Pélissier<sup>1</sup>,  
Jean-Philippe Gastellu-Etchegorry<sup>3</sup>, Eloi Grau<sup>3</sup> and Pierre Couteron<sup>1</sup>

<sup>1</sup>*Institut de Recherche pour le Développement (IRD), UMR AMAP*

<sup>2</sup>*Institut National de la Recherche Agronomique (INRA), UMR AMAP*

<sup>3</sup>*Université Paul Sabatier, UMR CESBIO  
France*

## 1. Introduction

The challenging task of biomass prediction in dense and heterogeneous tropical forest requires a multi-parameter and multi-scale characterization of forest canopies. Completely different forest structures may indeed present similar above ground biomass (AGB) values. This is probably one of the reasons explaining why tropical AGB still resists accurate mapping through remote sensing techniques. There is a clear need to combine optical and radar remote sensing to benefit from their complementary responses to forest characteristics. Radar and Lidar signals are rightly considered to provide adequate measurements of forest structure because of their capability of penetrating and interacting with all the vegetation strata.

However, signal saturation at the lowest radar frequencies is observed at the midlevel of biomass range in tropical forests (Mougin et al. 1999; Imhoff, 1995). Polarimetric Interferometric (PolInSAR) data could improve the inversion algorithm by injecting forest interferometric height into the inversion of P-band HV polarization signal. Within this framework, the TROPISAR mission, supported by the Centre National d'Etudes Spatiales (CNES) for the preparation of the European Space Agency (ESA) BIOMASS program is illustrative of both the importance of interdisciplinary research associating forest ecologists and physicists and the importance of combined measurements of forest properties.

Lidar data is a useful technique to characterize the vertical profile of the vegetation cover (e.g. Zhao et al. 2009) which in combination with radar (Englhart et al. 2011) or optical (e.g. Baccini et al. 2008; Asner et al. 2011) and field plot data may allow vegetation carbon stocks to be mapped over large areas of tropical forest at different resolution scales ranging from 1 hectare to 1 km<sup>2</sup>. However, small-footprint Lidar data are not yet accessible over sufficient extents and with sufficient revisiting time because its operational use for tropical studies remains expensive.

At the opposite, very-high (VHR) resolution imagery, i.e. approximately 1-m resolution, provided by recent satellite like Geoeye, Ikonos, Orbview or Quickbird as well as the forthcoming Pleiades becomes widely available at affordable costs, or even for free in certain regions of the world through Google Earth®. Compared to coarser resolution imagery with

1 pixel size greater than 4 meters, VHR imagery greatly improves thematic information on forest  
2 canopies. Indeed, the contrast between sunlit and shadowed trees crowns as visible on such  
3 images (Fig. 1) is potentially informative on the structure of the forest canopy while new  
4 promising methods now exist for analyzing these fine scale satellite observations (e.g.  
5 Bruniquel-Pinel & Gastellu-Etchegorry, 1998; Malhi & Roman-Cuesta, 2008; Rich et al. 2010).  
6 Besides, we believe that there is also a great potential in similarly using historical series of  
7 digitized aerial photographs that proved to be useful in the past for mapping large extents of  
8 unexplored forest (Le Touzey, 1968; Richards, 1996) for quantifying AGB changes through time.  
9 This book chapter presents the advancement of a research program undertaken by our team  
10 for estimating high biomass mangrove and *terra firme* forests of Amazonia using canopy  
11 grain from VHR images (Couteron et al. 2005; Proisy et al. 2007; Barbier et al., 2010; 2011).  
12 We present in a first section, the canopy grain notion and the fundamentals of the Fourier-  
13 based Textural Ordination (FOTO) method we developed. We then introduce a dual  
14 experimental-theoretical approach implemented to understand how canopy structure  
15 modifies the reflectance signal and produces a given texture. We discuss, for example, the  
16 influence of varying sun-view acquisition conditions on canopy grain characteristics. A  
17 second section assesses the potential and limits of the canopy grain approach to predict  
18 forest stand structure and more specifically above ground biomass. Perspectives for a better  
19 understanding of canopy grain-AGB relationships conclude this work.  
20



21  
22 Fig. 1. Differences of canopy grain perception between two 300 m square subset images of  
23 different spatial resolution over a mixed savanna forest-inhabited area, French Guiana. Left:  
24 a 2.5-m SPOT5 Fusion image acquired in October 2010. Right: a 20-cm aerial photograph  
25 acquired in July 2010 (© L'Avion Jaune).

## 26 2. The canopy grain approach

### 27 2.1 Notion of canopy grain

28 The notion of canopy grain needs to be clarified. In the context of this study, it refers to the  
29 aspect of the uppermost layer of the forest, i.e. the top canopy. It emerges from the images

1 as soon as the contrast between sunlit and shadowed tree crowns becomes perceptible. This  
2 property increases with the fineness of image spatial resolution (Fig. 1) that explains why, in  
3 VHR images, the tropical forest no longer appears as a continuous homogenous layer, or  
4 'red carpet', as it is the case on medium resolution images with pixel size greater than 5  
5 meters (Fig. 1). Intuitively, the canopy grain depends on both the spatial distribution of trees  
6 within a scene and the shapes and dimensions of their crowns. The question is then how to  
7 derive quantitative measurements of such canopy grain texture. Following Rao and Lohse  
8 (1993), who explained that repetitiveness is the most important dimension of human  
9 perception for structural textures, our idea is to measure the degree of repetitiveness  
10 expressed in canopy grain within a forest scene. Two dimensional (2D) Fourier or wavelet  
11 transforms proved to be well adapted for this purpose (e.g. Couteron, 2002; Ouma et al.,  
12 2006) because they allow shifting canopy grain properties from the spatial domain to the  
13 frequency domain. Though of potential larger application, we focus in this paper on the 2D  
14 Fourier-based frequency spectra as a mean for relating tropical forest canopy grain to above-  
15 ground biomass (AGB).

## 16 2.2 The FOTO method

### 17 2.2.1 Workflow up to forest AGB prediction

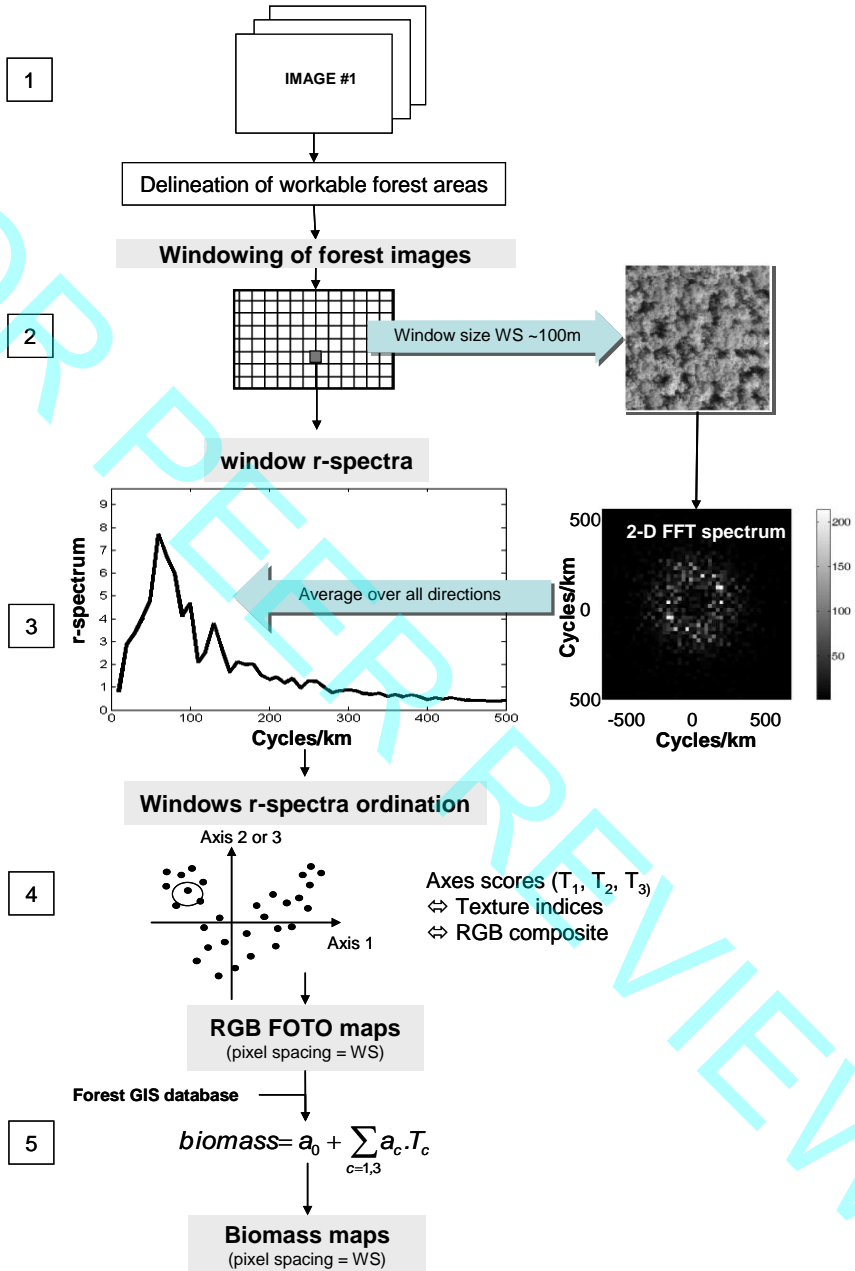
18 The well-known Fourier transform is highly suitable for analyzing repetitiveness of canopy  
19 grain as it breaks down an intensity signal into sinusoidal components with different  
20 frequencies. We built on this principle the development of the Fourier-based Textural  
21 Ordination (FOTO) method to primarily explore the potential of digitized aerial  
22 photographs and VHR satellite images for predicting tropical forest stand structure  
23 parameters including AGB (Couteron et al., 2005; Proisy et al. 2007). We summarize,  
24 hereafter, the flow of operations that yield AGB predictions from FOTO outputs.

25 A prerequisite of the method is to mask non-forest areas, such as clouds and their shadows,  
26 water bodies, savannas, crops and civil infrastructures areas (Fig. 2, step 1). The method  
27 then proceeds with the specification of a square window size in which 2D-Fourier spectra  
28 are computed (Fig. 2, step 2). To be clear, the window size  $WS$  is expressed in meters as:

$$29 \quad \quad \quad WS = N \cdot \Delta S \quad \quad \quad (1)$$

30 where  $N$  is the number of pixels in the X or Y direction of the image and  $\Delta S$  is the pixel size  
31 in meters.  $WS$  may influence the FOTO results as discussed in the following sub-section.  
32 Using large  $WS$  also means that spatial resolution of the FOTO outputs and subsequent  
33 biomass maps will be  $N$  times coarser than the spatial resolution of the source image(s).  
34 Although the use of a sliding window is computationally intensive, it can attenuate the  
35 effects of both spatial resolution degradation and study areas fringe erosion.

36 After windowing the forest images, Fourier radial spectra (or r-spectra) are computed and  
37 give for each window, the frequency vs. amplitude of a sinusoidal signal that fits the spatial  
38 arrangement of pixels grey levels (Fig. 2, step 3) as described in the next paragraph. The r-  
39 spectra may be then stacked into a common matrix in which each row corresponds to the r-  
40 spectrum of a given window, whereas each column contains amplitude values. This table is  
41 then submitted to multivariate analysis techniques (ordinations/classifications). With this  
42 approach, the study can concern as many images as necessary, providing they have the  
43 same spatial resolution. The resulting table can, for instance, be submitted to a standardized  
44 principal component analysis (PCA; Fig. 2, step 4). Window scores on the 3 most prominent

1  
23  
4

5 Fig. 2. Flow of operations involved in the FOTO analysis up to biomass prediction

1 axes are used as texture indices (the so-called FOTO indices) that are mapped by composing  
2 red-green-blue (RGB) images expressing window scores values against first, second and  
3 third axes, respectively. Such FOTO maps have a spatial resolution equal to the window size  
4  $WS$ . The final step (Fig. 2, step 5) is to relate ground truth forest plot biomass to FOTO  
5 indices using a linear model of the form:

$$6 \quad AGB = a_0 + \sum_{c=1}^3 a_c T_c \quad (2)$$

7 where  $a_0$  and  $a_c$  are the coefficients of the multiple regression of  $AGB$  onto the texture indices  
8  $T$  obtained from the first three PCA axes.

### 9 **2.2.1 Computing radial spectra of forest plots**

10 The computation of radial spectra has to be detailed because such frequency signatures are  
11 essential components of the canopy grain analysis. It is to note that the calculation of r-  
12 spectra is also possible for any single image extract centered on one forest plot as illustrated  
13 in the numerous examples provided hereafter.

14 Each image extract is subjected to the two dimensional discrete fast Fourier transform  
15 algorithm implemented in most of the technical computing software. Image intensity  
16 expressed in spatial  $XY$  Cartesian referential domain is transposed to the frequency domain.  
17 Power spectrum decomposing the image variance into frequency bins along the two Cartesian  
18 axes is then obtained for each square window (Fig. 2, step 3, right). This latter was  
19 demonstrated as an efficient way to quantify pattern scale and intensity (Couteron et al. 2006)  
20 from images of various vegetation types (Couteron et al. 2002; 2006). Assuming that images of  
21 tropical forest have isotropic properties, the radial spectra are then obtained after azimuthally  
22 averaging over all travelling directions (Fig. 2, step 3, left). Frequencies are expressed in cycles  
23 per kilometer, i.e. the number of repetitions over a 1 km distance. The discrete set of spatial  
24 frequencies  $f$  can be also transformed into sampled wavelengths (in meters) as  $\lambda=1000/f$ . For  
25 example, a frequency of 200 cycles per kilometre corresponds to a wavelength of 5 metres.

### 26 **2.2.2 Principal component analysis for regional analysis**

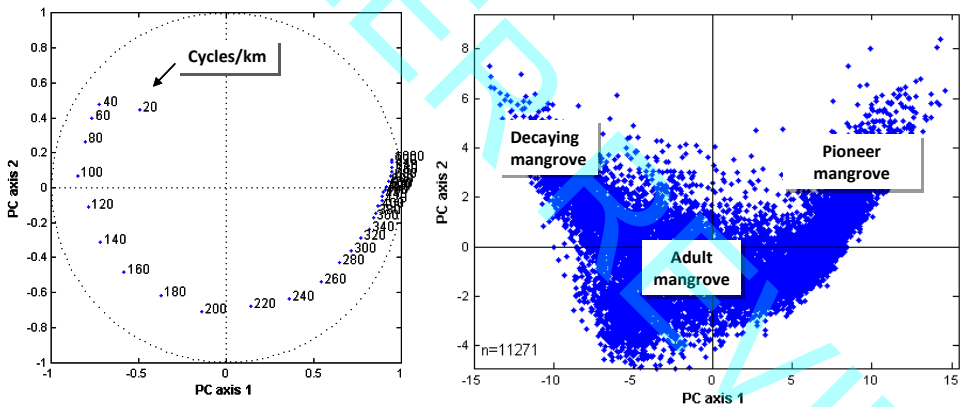
27 Standardized principal component analysis of the spectra table created by the stacking of all  
28 r-spectra is a mean to perform regional analysis of canopy grain variations through one or  
29 several image scenes. For illustration, a 0.5-m panchromatic Geoeye image covering (after  
30 masking non-forest areas) 11271 hectares of mangroves is analyzed (Fig. 3). The three first  
31 factorial axes of the PCA accounted for more than 81% of the total variability. The first PCA  
32 axis opposes coarse and fine canopy grain that correspond to spatial frequencies of less than  
33 100 cycles/km ( $\lambda=10$  m) and more than 250 cycles/km ( $\lambda=4$  m), respectively. Intermediate  
34 spatial frequencies are found with high negative loadings on the second axis.

35 From this analysis, we coded window scores on the three main PCA axes as RGB real values  
36 (Fig. 4). Pioneer and young stages of mangroves are characterized by red-i.e. high scores on  
37 PC1 only- whereas intergrades between blue and cyan corresponded to areas with adult  
38 trees (low positive scores on PC1 and negative scores on PC2). Green color maps mature and  
39 decaying stages of mangrove with high PC2 and very low PC1 scores. Hence,  
40 coarseness/fineness gradients of thousands of unexplored hectares of mangrove can be  
41 mapped and allow to capture, at a glance, the overall spatial organization presented in the

1 image. An equivalent result was also obtained using a 1-m panchromatic Ikonos image  
 2 (Proisy et al. 2007). The FOTO analysis is confirmed of prime interest for mangrove  
 3 monitoring studies and for highlighting coastal processes in French Guiana (Fromard et al.  
 4 2004) through the mapping of forest growth stages.

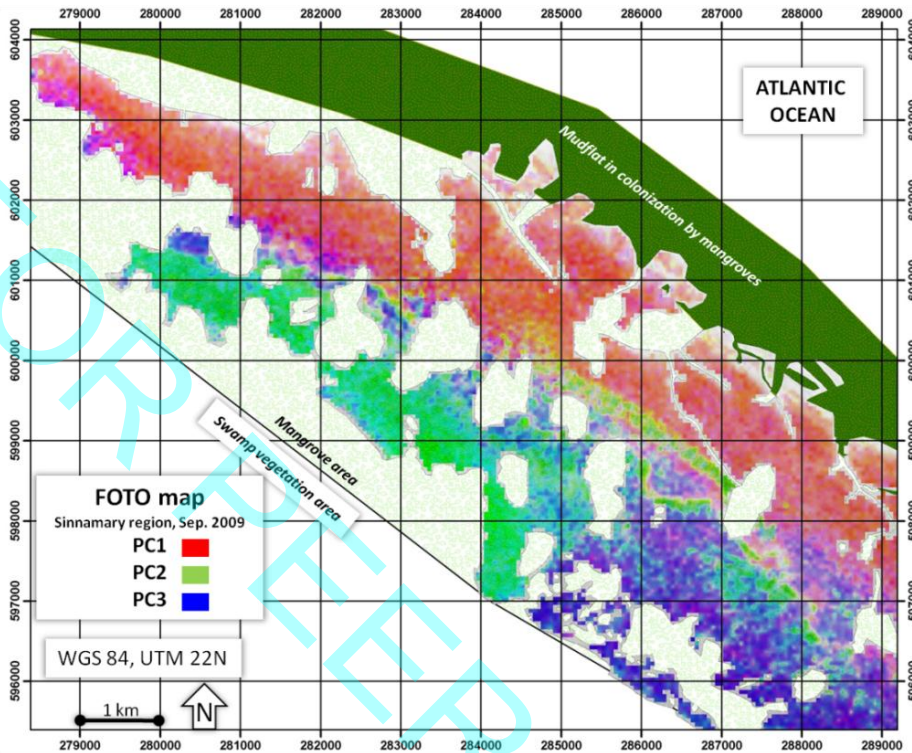
### 5 **2.3 The DART modelling method**

6 Large-scale validation of the FOTO method is highly desirable, to study both the method's  
 7 sensitivity to complex variations in forest structure and to instrumental perturbations.  
 8 However, it is notoriously difficult to obtain both detailed forest structure information in  
 9 inaccessible tropical environments and cloudless imagery over field plots. It was therefore  
 10 necessary to develop a modeling framework for testing FOTO sensitivity, in simplified but  
 11 controlled conditions (Barbier et al. 2010; 2011; in press).



21  
 22  
 23  
 24  
 25  
 26  
 27  
 28  
 29

30 Fig. 3. Principal component analysis of Fourier spectra obtained from the FOTO analysis of a  
 31 Geoye panchromatic image covering 11271 hectares of mangroves in French Guiana.  
 32 Correlation between PCA axes and spatial frequencies are shown in the left graph.



1  
2 Fig. 4. Panchromatic-derived FOTO map obtained from a Geosyde panchromatic image  
3 acquired in September 2009. RGB channels code for windows scores on PCA axes. A large  
4 part of the mangrove area is masked because either under clouds or with bare mud.

### 5 2.3.1 Basic principles

6 The 3D Discrete Anisotropic Radiative Transfer (DART) model is a ray-tracing model that  
7 can simulate, simultaneously in several wavelengths of the optical domain, remotely sensed  
8 images of heterogeneous natural and urban landscapes with or without relief, using 3D  
9 generic representations of these landscapes for any sun direction, any view direction or any  
10 atmosphere (Gastellu-Etchegorry et al., 2004). The model is freely downloadable from  
11 <http://www.cesbio.uvsq.fr/fr/dart.html> for scientific studies, after signing a charter of use. In  
12 the case of forests, a DART scene, namely a 'masket', is a three-dimensional representation of  
13 a forest stand within a voxel space. Transmittance and phase functions (the optical  
14 properties) associated to each voxel depend on the voxel type (leaves, trunk, soil, etc.).  
15 Leaves cells are modelled as turbid media with volume interaction properties whereas  
16 others voxel types are taken as solid media with surface properties. Others structural  
17 characteristics within the cell (e.g. LAI, leaf and branches angle distribution) can be taken  
18 into account. The scattering of rays from each cell is simulated iteratively in a discrete  
19 number of directions. We keep the masket size 10% larger of the FOTO window or the forest  
20 plot sizes in order to avoid border effects. The final DART image is a sub-scene of  
21 dimensions equal to the reference window or plot.

### 2.3.2 3D forest templates

A first step within this modeling framework is to reproduce biologically realistic 3D templates of forests. Depending on the level of detail and biological realism one is to obtain, different approaches can be considered to build 3D forest mock-ups. For instance, the Stretch model (Vincent & Arja, 2008) allows accounting for dynamic crown deformations through various mechanisms and levels of plant plasticity. However, for our present purpose, we focus on variations in size-frequency distributions of trees, without entering too much into architectural (i.e. structural and dynamic) details. For this reason, we developed the Allostand model (Barbier et al. in press), a simple Matlab® algorithm using a DBH distribution, established DBH-Crown-height allometric relationships, and an iterative hard-core point process generator, to reproduce 'lollipop stands', that is a 3D arrangement of trunk cylinders bearing ellipsoid crowns. This forest template matches the DART market requirements, e.g. a list of trees with parameters of their 3D geometry. Such simulation framework is particularly well adapted to the study of mangroves forest in which few species grow rapidly over areas with no relief (Fig. 5).

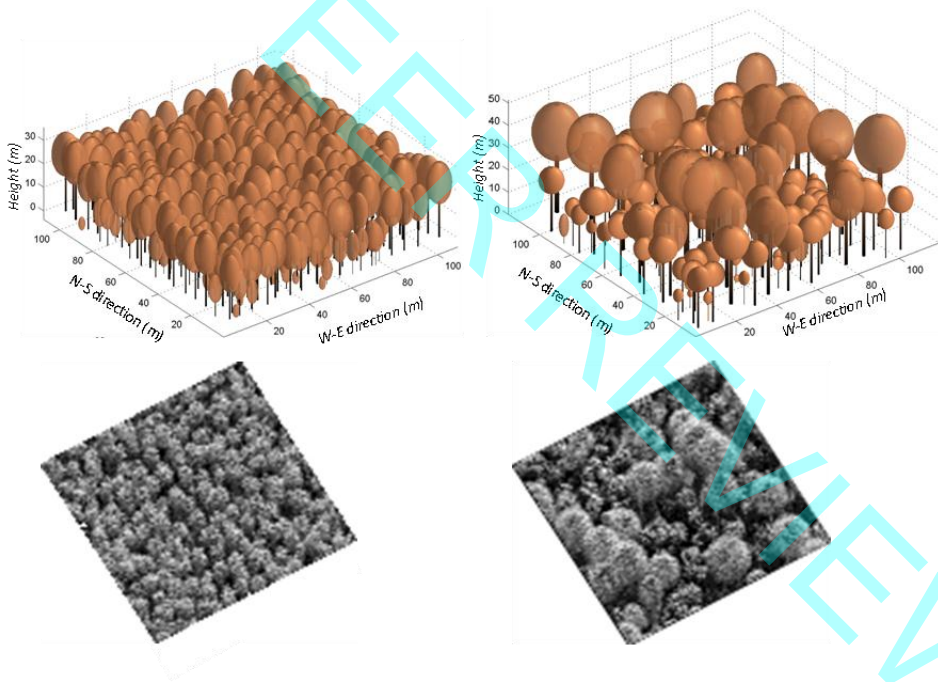


Fig. 5. Examples of 110 × 110m mockups obtained for a young *Avicennia* mangrove of 159 tDM.ha<sup>-1</sup> (top left) and a mixed adult mangrove of 360 tDM.ha<sup>-1</sup> (top right). Associated 1-m pixel DART images simulated at 0.75 μm are shown below.

### 2.3.3 Virtual canopy images

In this work, we only simulated mono-spectral images in the visible domain on flat topography without taking into account atmospheric effects (Fig. 5). Standard optical profiles of reflectance for soil, trunks and leaves are selected from the DART database using, for instance, '2D soil-vegetation', '2D bark\_spruce' and '3D leaf\_deciduous' files. Such oversimplified images of virtual forest stands composed of trees with 'lollipop-shaped' crowns produce homogeneous texture dominated by few frequencies. The FOTO analysis of 330 DART images however demonstrated their potential for benchmarking textural gradient of real forest canopies throughout the Amazon basin (cf. Fig. 3 in Barbier et al. 2010).

## 2.4 Influence of instrumental characteristics

### 2.4.1 Window size and spatial resolution

Large windows may include features characterizing landforms such as relief variations rather than canopy grain (Couteron et al., 2006) whereas small windows may be unable to adequately capture large canopy features observable in mature growth stages. However, whatever the window size taken within a reasonable range of variations, i.e. 75 to 150 m for tropical forest, spatial frequencies should display more or less the same patterns of contribution to PCA axes (Couteron et al. 2006). The influence of spatial resolution on the sensitivity of r-spectra to capture canopy grain of different forest types was highlighted using 1-m panchromatic and 4-m near infrared (NIR) Ikonos images in Proisy et al. (2007).

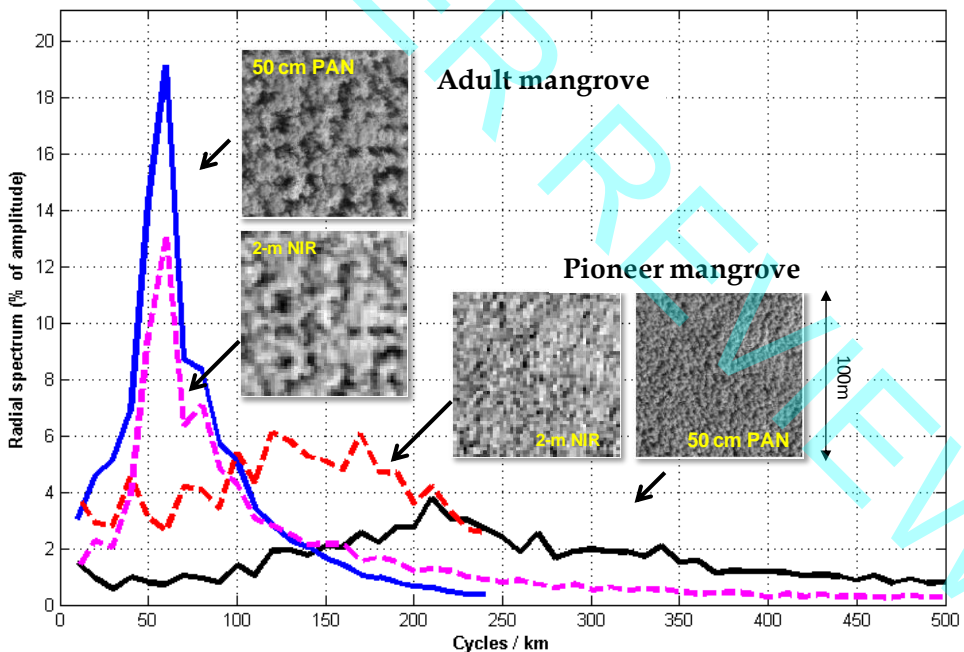
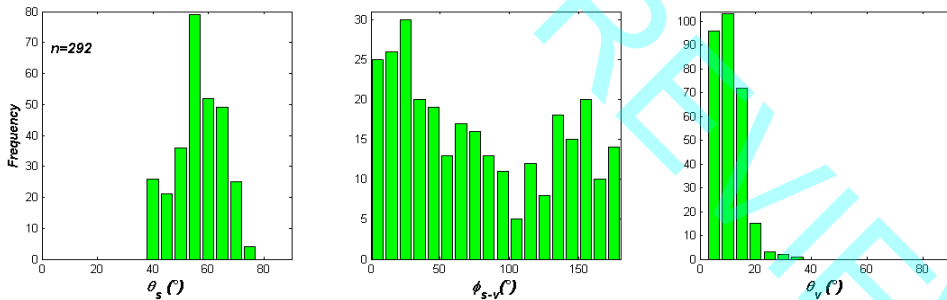


Fig. 6. Radial spectra of 2 different mangrove growth stages using 0.5-m and 2-m panchromatic and near infrared Geoeye channels.

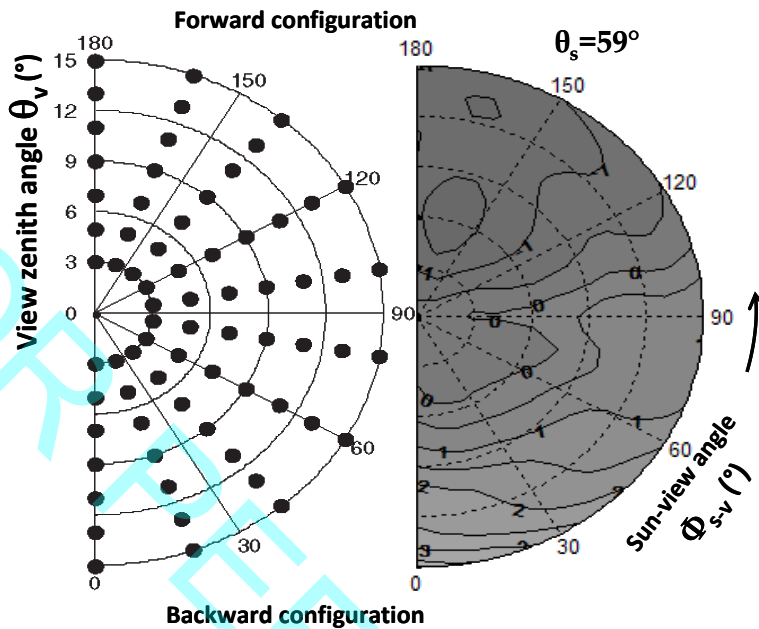
1 The loss of sensitivity to the finest textures was also observed using 2-m NIR channel of  
 2 Geoeye image (Fig. 6). Whereas r-spectra of 0.5-m and 2-m image extracts displayed the  
 3 same behaviour with an identical dominant frequency, they did not exhibit the same  
 4 profiles for the pioneer stage consisting of a very high density of trees with 2-3 m crown  
 5 diameters. This limitation was also observed for the same forest growth stages after  
 6 comparison of 1-m and 4-m Ikonos channels (see Fig. 4 in Proisy et al. 2007). As the  
 7 limitation with regard to the youngest stages appeared using 2-m channels, it was  
 8 recommended to privilege the use of panchromatic satellite images with metric and sub-  
 9 metric pixels.

#### 10 2.4.2 Sun and viewing angles: the BTF

11 Parameters of VHR image acquisitions such as sun elevation angle  $\theta_s$ , viewing angle from  
 12 nadir  $\theta_v$  and azimuth angle  $\Phi_{s-v}$  between sun and camera can vary significantly as illustrated  
 13 in Fig. 7. We introduced the bidirectional texture function (BTF; Barbier et al. 2011) diagrams  
 14 to map the influence of different acquisitions conditions in terms of texture perception (Fig.  
 15 8). The finest textures are perceived in the sun-backward configuration whereas the coarsest  
 16 are observed when sun is facing the camera (the forward configuration) due to the loss of  
 17 perception in shadowed areas. These findings show that to ensure a coherent comparison  
 18 between scenes, one must either use images with similar acquisition conditions, or use a BTF  
 19 trained on similar forest areas or derived from a sufficiently realistic physical simulations to  
 20 allow minimizing these effects (Barbier et al. 2011).



27  
 28  
 29  
 30  
 31  
 32  
 33 Fig. 7. Variation of acquisition parameters through a dataset of 292 images. The dataset  
 34 includes 270 Quickbird, 8 Geoeye, 9 Ikonos and 5 Orbview images acquired over tropical  
 35 forest of Bangladesh, Brazil, Cameroun, Central African Republic, French Guiana, India,  
 36 Indonesia, Democratic Republic of Congo.



1  
 2 Fig. 8. Example of discrete sampling of  $\theta_v$  and  $\Phi_{s-v}$  acquisition angles with  $\theta_s = 59^\circ$  (left) to  
 3 generate the Bidirectional Texture Function (BTF). The BTF diagram (right) is computed  
 4 from the mean PC1 scores resulting from the FOTO analysis of numerous DART images and  
 5 3D forest templates. Brighter intensities values imply finer perceived canopy textures.

### 6 3. From canopy grain to AGB

#### 7 3.1 Requirements for forest data

8 The canopy grain approach must be calibrated at the forest plot scale i.e. by conducting  
 9 forest inventories from which above ground biomass will be estimated. Areas of about  
 10 one hectare are necessary to take into account structural diversity within the forest plot.  
 11 This area of inventory can possibly be reduced for simpler forest stands and plantations,  
 12 but this is basically dependent on the size of the canopy trees since the computation of  
 13 FOTO indices should be meaningful at plot scale (Couteron et al. 2005). AGB estimation  
 14 for each plot will be taken as the AGB of reference to correlate with FOTO indices. Since  
 15 very labor-intensive destructive measures are necessary to acquire biomass values,  
 16 reference field AGB values are generally computed indirectly using pre-established  
 17 allometric functions predicting tree AGB from the measure of the tree diameter at breast  
 18 height (DBH) as explained, for example, by Chave et al. (2005). On this basis prediction of  
 19 stand AGB in reference field plots can be computed by measuring DBH > 5 cm in young  
 20 forest and DBH > 10 cm in adult forest. Allometric equation between DBH and tree biomass  
 21 are established from few cut trees that are weighed on site (e.g. Fromard et al. 1998 for  
 22 mangroves and Brown et al, 1989 for tropical moist forest). Due to the extreme difficulty  
 23 of achieving this kind of field work, relationships are often limited to trees with  
 24 DBH < 40 cm whereas DBH histograms in tropical forest show values above 150 cm.

1 Additionally, for a given species varying tree heights and crowns dimensions may yield  
2 important mass differences that the parsimonious relationships cannot take into account.  
3 Selecting an appropriate allometric model is then crucial and the sampling uncertainty  
4 relative to the size of the study plot should also be addressed carefully (e.g. Chave et al.  
5 2004).

6 Tree location, crown shape, tree height and wood specific gravity also constitute useful  
7 information that will contribute to the characterization of the forest structure typology.  
8 Although it remains unrealistic in heterogeneous forests without the help of skilled  
9 botanists, identification of tree species is advisable in low-diversified situations, since the  
10 inclusion of a specific wood gravity parameter into allometric equations proved to improve  
11 significantly the model (Chave et al. 2005). Such additional data will also be valuable for  
12 initializing 3D forest templates. It is important to note that, in tropical forest, tree height  
13 measurements from the ground are problematic and cumbersome explaining the  
14 enthusiasm aroused by Lidar data (e.g. Gillespie et al. 2004). Another important point to  
15 improve AGB prediction would be to conduct forest inventories simultaneously to image  
16 acquisitions.

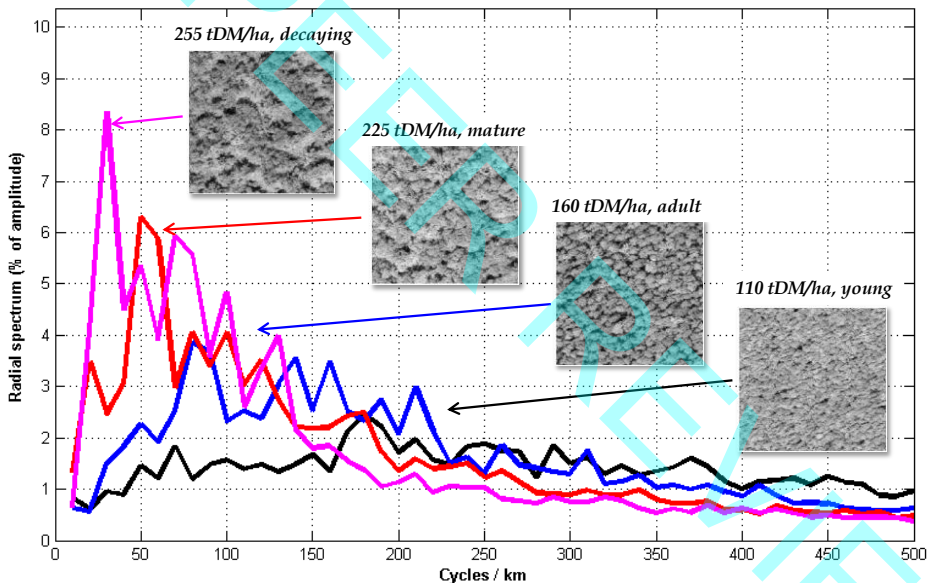
### 17 **3.2 Sensitivity to forest structure and AGB**

18 Assuming that the constituted forest plots dataset is well distributed within the acquired  
19 scene(s), Fourier r-spectra can be computed for windows centred on each plot. For  
20 example, when applied to 1-m Ikonos (Proisy et al. 2007) or 0.5-m Geoeye panchromatic  
21 images (Fig. 9) r-spectra permit good discrimination of a wide array of canopy structures  
22 of mangroves (Fig. 9). Furthermore pre-adult, mature and decaying mangrove forests  
23 show contrasted signatures with dominant frequencies around 180, 80, 50 and 30 cycles  
24 per kilometre.

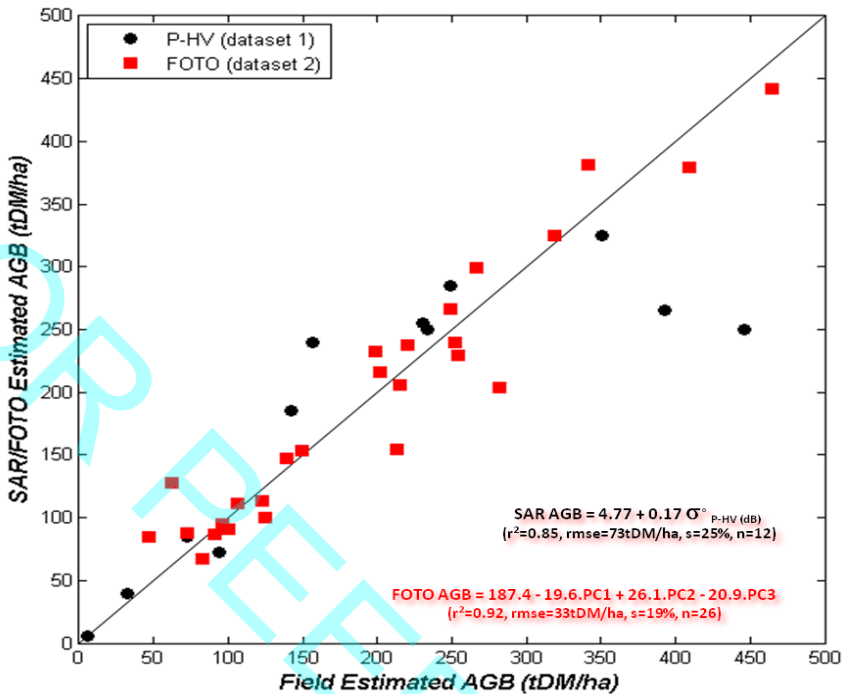
25 Inverting FOTO indices (the three first PCA axes) into AGB of forest plots distributed  
26 over two different sites (i.e. two different images) yielded good correlations and low  
27 errors, as presented in Fig. 10. Compared to estimations provided by the P-band HV  
28 polarisation channel, FOTO-derived AGB did not show saturations over the whole range  
29 of mangrove biomass (Fig. 9), i.e. up to 500 tDM.ha<sup>-1</sup> and rmse error remains acceptable  
30 (33 tDM.ha<sup>-1</sup>). This result suggests that, in the case of closed canopies with sub-strata of  
31 low biomass (e.g. the mangrove ecosystem in French Guiana), the canopy grain approach  
32 is suitable to map AGB because crown size and spatial distribution are directly  
33 correlated to standing biomass of the dominant trees. However, one do not forget that  
34 the remote sensing-based model of AGB is assessed with respect to allometric  
35 predictions of "true" AGB, i.e. the aboveground dry mass of trees, from dendrometric  
36 data, so that the quality of the allometric model is potentially a additional source of bias  
37 (Chave et al. 2004; 2005).

38 Assuming the constituted forest dataset is well distributed within the acquired scene(s)  
39 r-spectra can be computed for Fourier windows centred on each plot. For example, when  
40 applied to 1-m Ikonos (Proisy et al. 2007) or 0.5-m Geoeye panchromatic images, r-  
41 spectra permit good discrimination of a wide array of forest structures of mangroves  
42 (Fig. 9). For young, pre-adult, mature and decaying mangrove forests, they show  
43 contrasted signatures with dominant frequencies around 180, 80, 50 and 30 cycles per  
44 kilometre.

1 Good correlations were obtained between the first axis and tree density ( $r^2=0.8$ ) or mean  
 2 quadratic DBH ( $r^2=0.71$ ) in tropical evergreen *terra firme* forest Coutron et al (2005).  
 3 However, forest heterogeneity and presence of relief makes the canopy approach to be  
 4 used carefully, that is one must analyze visually whether the relief influences or not some  
 5 of the PCA axes (e.g. Ploton, 2010). Only axes immune to relief influence should be used  
 6 for biomass prediction otherwise the result may be biased or highly context-dependent.  
 7 Moreover, due to the diversity of forest stand structures in tropical *terra firme* forests, a  
 8 sufficient number of studies in diversified locations and contexts are still needed before  
 9 general conclusions can be reached about the robustness of such correlations.  
 10 Independent ongoing studies suggest that the correlation with density is highly context-  
 11 specific while the correlation with the mean quadratic diameter may be a more robust  
 12 feature.



18  
 19  
 20  
 21  
 22  
 23  
 24 Fig. 9. Radial spectra and associated 100 x 100 m images of different mangrove growth  
 25 stages using a 0.5 m panchromatic Geoeye image acquired in 2009. Forest inventories dated  
 26 of 2010 and 2011. Note the r-spectra of the open canopy decaying stage. A photograph of  
 27 this plot is available in Fig. 11.



1  
2 Fig. 10. Comparison of FOTO- (Proisy et al. 2007) and P-HV-derived (from Mougin et al.  
3 1999) biomass estimates in mangroves of French Guiana

### 4 3.3 Present limitations of the methods and prerequisite

5 In tropical forest, both gaps and multi-strata organization are often observed. Gaps are due  
6 to accidental tree falls or natural decaying of some canopy trees (Fig. 11, left). In presence of  
7 gaps, r-spectra tend to be skewed towards low frequencies and this may be erroneously  
8 interpreted as if the canopy contained large tree crowns (Fig. 9, r-spectrum of the decaying  
9 stage). In fact, gap-influenced r-spectra cannot be automatically related to the same biomass  
10 levels and must be removed from the PCA analysis to avoid biases in the AGB-FOTO  
11 relationship. Identically, the method was so far tested principally on evergreen forests.  
12 Further studies are needed regarding deciduous forests, not only because of the seasonal  
13 changes of the canopy aspect, but also because biomass of understorey vegetation often  
14 found in such forest type is not necessarily negligible. As spectral properties of the  
15 understorey may influence the overall reflectance of the corresponding pixels, this may be  
16 all more confusing if there is no intermediate stratum beneath the highest deciduous trees.  
17 An example of this is provided by the so-called *Maranthaceae* forest in Africa (Fig. 11, right)  
18 which presents a fairly closed albeit deciduous canopy and a very scarce intermediate tree  
19 storey. Such a structure allows the development of a dense herbaceous cover. Without  
20 relevant field information, results of the FOTO approach may be confusing in those forests.  
21 Their standing biomass is probably less than for evergreen closed forests since woody  
22 intermediate storey is missing, whereas both canopies are dominated by trees with large  
23 crowns. At least, statistical relationships between FOTO indices and AGB should be

1 analyzed after separating deciduous and evergreen forests than may be simultaneously  
2 present in a given region. Appropriate regional pre-stratification using multispectral  
3 satellite data and/or L- or P-band polarized signatures (Proisy et al. 2002) may help towards  
4 this purpose.  
5



6  
7 Fig. 11. Two examples of specific forest structures for which canopy grain and total AGB  
8 relationships cannot be safely derived without prior-stratification of the main forest types.  
9 Left: Decaying mangrove, with both large surviving trees and large canopy gaps, French  
10 Guiana © C. Proisy. Right: *Maranthaceae* understory, overtopped by a fairly continuous  
11 albeit deciduous forest canopy referred to as “*Maranthaceae* forests” in Cameroun, Africa,  
12 note the absence of any intermediate tree strata © N. Barbier.

#### 13 4. Conclusion

14 The canopy grain approach is largely original. It combines common techniques, i.e. Fourier  
15 transform and principal component analysis to characterize tropical canopy aspect and  
16 beyond forest structure from images of metric resolution. It can be implemented without  
17 prior radiometric correction, such as reflectance calibration or histogram range concordance.  
18 Regarding the increasing availability of metric to sub-metric optical images, the FOTO  
19 canopy grain analysis demonstrated its potential to capture gradients of forest structural  
20 characteristics in tropical regions. Within this context, the possible contribution of the  
21 canopy grain approach to the challenging task of estimating tropical above-ground biomass  
22 is worth being assessed at very broad scale. Such aim requires conducting simultaneously  
23 observational and simulation studies aiming at better understanding how canopy grain is  
24 sensitive to forest structure or biomass in various types of forests under various conditions  
25 of image acquisitions. There is particularly an important field of research in simulating  
26 multi-spectral and metric reflectance images from realistic forest 3D templates to identify,  
27 for instance, the range of conditions for which inverting above ground biomass of tropical  
28 forests appears possible. Considering the extreme complexity of most the tropical forests, it  
29 would be illusory to believe that only one remote sensing technique can provide all the  
30 information required to the AGB inversion. We thus believe that combining canopy grain  
31 analysis with low frequencies radar-based studies can provide new insights on this problem.

## 5. Acknowledgment

This work is supported by the Centre National d'Etudes Spatiales (CNES) for the preparation of the 'Pleiades' mission and joins the *Infolittoral-1* project funded by the French "Unique Inter-ministerial Fund" and certified by the "Aerospace Valley competitiveness cluster" (<http://infolittoral.spotimage.com/>). Nicolas Barbier has a Marie Curie (UE/IEF/FP7) grant. Research in central Africa is supported by the *Programme Pilote Régional* (PPR FTH-AC) of IRD. We thank J-L. Smock and Michel Tarcy for their strong motivation in mangrove field measurements. We also thank Bruno Roux and Michel Assenbaum for their kind support in providing us for free several Avion Jaune© images (<http://www.lavionjaune.fr>).

## 6. References

- Asner, G. P., G. V. N. Powell, J. Mascaro, D. E. Knapp, J. K. Clark, J. Jacobson, T. Kennedy-Bowdoin, A. Balaji, G. Paez-Acosta, E. Victoria, L. Secada, M. Valqui and R. F. Hughes High-resolution forest carbon stocks and emissions in the Amazon. *Proceedings of the National Academy of Sciences* Vol.107, No.38 (September 2010), pp.16738-16742, ISSN: 1091-6490
- Baccini, A., Laporte, N., Goetz, S. J., Sun, M. & Dong, H. (2008). A first map of tropical Africa's above-ground biomass derived from satellite imagery *Environmental Research Letters*, Vol.3, No.4, (October-December 2008), pp.1:9, ISSN: 1748-9326
- Barbier, N., Couteron, P., Proisy, C., Malhi, Y. & Gastellu-Etchegorry, J.-P. (2010). The variation of apparent crown size and canopy heterogeneity across lowland Amazonian forests. *Global Ecology and Biogeography*, Vol.19, No.1, (January 2010), pp.72-84, ISSN 1466-8238
- Barbier, N., Proisy, C., Véga, C., Sabatier, D. & Couteron, P. (2011). Bidirectional texture function of high resolution optical images of tropical forest: An approach using LiDAR hillshade simulations. *Remote Sensing of Environment*, Vol.115, No.1, (January 2011), pp.167-179, ISSN 0034-4257
- Barbier, N., Couteron, P., Gastellu-Etchegorry, J. P. & Proisy, C. (xxxx). Linking canopy images to forest structural parameters: potential of a modeling framework. *Annals of Forest Science*, In press, ISSN: 1297-966X
- Brown, S., Gillespie, A. J. R. & Lugo, A. E. (1989). Biomass estimation methods for tropical forests with applications to forest inventory data. *Forest Science*, Vol.35, No.4, (December 1989), pp.881-902, ISSN : 0015-749X
- Bruniquel-Pinel, V. & Gastellu-Etchegorry, J. P. (1998). Sensitivity of Texture of High Resolution Images of Forest to Biophysical and Acquisition Parameters. *Remote Sensing of Environment*, Vol.65, No.1, (July 1998), pp.61-85, ISSN: 0034-4257
- Chave, J., Condit, R., Aguilar, S., Hernandez, A., Lao, S. & Perez, R. (2004). Error propagation and scaling for tropical forest biomass estimates. *Philosophical Transactions of the Royal Society of London, Series B*, Vol.359, (March 2004), pp.409-420, ISSN: 0962-8436
- Chave, J., Andalo, C., Brown, S., Cairns, M. A., Chambers, J. Q., Eamus, D., Folster, H., Fromard, F., Higuchi, N., Kira, T., Lescure, J.-P., Nelson, B. W., Ogawa, H., Puig, H., Riéra, B. & Yamakura, T. (2005). Tree allometry and improved estimation of

- 1 carbon stocks and balance in tropical forests. *Oecologia*, Vol.145, No.1, (August  
2 2005), pp.87-99, ISSN: 1432-1939
- 3 Couteron, P. (2002). Quantifying change in patterned semi-arid vegetation by Fourier  
4 analysis of digitized aerial photographs. *International Journal of Remote Sensing*,  
5 Vol.23, No.17, (October 2002), pp.3407-3425, ISSN: 1366-5901
- 6 Couteron, P., Pélissier, R., Nicolini, E. & Paget, D. (2005). Predicting tropical forest stand  
7 structure parameters from Fourier transform of very high-resolution remotely  
8 sensed canopy figures. *Journal of Applied Ecology*, Vol.42, No.6, (December 2005),  
9 pp.1121-1128, ISSN: 1365-2664
- 10 Couteron, P., Barbier, N. & Gautier, D. (2006). Textural ordination based on Fourier spectral  
11 decomposition: a method to analyze and compare landscape patterns. *Landscape  
12 Ecology*, Vol.21, No.4, (May 2006), pp.555-567, ISSN: 1572-9761
- 13 Fromard, F., Vega, C. & Proisy, C. (2004). Half a century of dynamic coastal change affecting  
14 mangrove shorelines of French Guiana. A case study based on remote sensing data  
15 analyses and field surveys. *Marine Geology*, Vol.208, No.2-4, (15 August 2004),  
16 pp.265-280, ISSN: 0025-3227
- 17 Enghart, S., Keuck, V. & Siegert, F. (2011). Aboveground biomass retrieval in tropical forests  
18 -- The potential of combined X- and L-band SAR data use. *Remote Sensing of  
19 Environment*, Vol.115, No.5, (May 2011), pp.1260-1271, ISSN: 0034-4257
- 20 Fromard, F., Puig, H., Mougouin, E., Marty, G., Betoulle, J. L. & Cadamuro, L. (1998). Structure,  
21 above-ground biomass and dynamics of mangrove ecosystems: new data from  
22 French Guiana. *Oecologia*, Vol.115, No.1, (June 1998), pp.39-53, ISSN: 0029-8549
- 23 Gastellu-Étchegorry, J. P., Martin, E. & Gascon, F. (2004). DART: a 3D model for simulating  
24 satellite images and studying surface radiation budget. *International Journal of  
25 Remote Sensing*, Vol.25, No.1, (January 2004), pp.73-96, ISSN: 0143-1161
- 26 Gillespie, T. W., Brock, J. & Wright, C. W. (2004). Prospects for quantifying structure,  
27 floristic composition and species richness of tropical forests. *International Journal of  
28 Remote Sensing*, Vol.25, No.4, (February 2004), pp.707-715, ISSN: 1366-5901
- 29 Imhoff, M. L. (1995). Radar backscatter and biomass saturation: ramifications for global  
30 biomass inventory. *IEEE Transactions on Geoscience and Remote Sensing*, Vol.33, No.2,  
31 (March 1995), pp.511-518, ISSN: 0196-2892
- 32 Letouzey, R. (1968), *Etude phytogéographique du Cameroun*. Lechevalier Eds., Paris.
- 33 Malhi, Y. & Román-Cuesta, R. M. (2008). Analysis of lacunarity and scales of spatial  
34 homogeneity in IKONOS images of Amazonian tropical forest canopies. *Remote  
35 Sensing of Environment*, Vol.112, No.5, (May 2008), pp.2074-2087, ISSN: 0034-4257
- 36 Mougouin, E., Proisy, C., Marty, G., Fromard, F., Puig, H., Betoulle, J. L. & Rudant, J. P. (1999).  
37 Multifrequency and multipolarization radar backscattering from mangrove forests.  
38 *IEEE Transactions on Geoscience and Remote Sensing*, Vol.37, No.1, (January 1999),  
39 pp.94-102, ISSN: 0196-2892
- 40 Ouma, Y. O., Ngigi, T. G. & Tateishi, R. (2006). On the optimization and selection of wavelet  
41 texture for feature extraction from high-resolution satellite imagery with  
42 application towards urban-tree delineation. *International Journal of Remote Sensing*,  
43 Vol.27, No.1, (January 10), pp.73-104, ISSN: 0143-1161
- 44 Ploton, P. 2010. Analyzing Canopy Heterogeneity of the Tropical Forests by Texture  
45 Analysis of Very-High Resolution Images - A Case Study in the Western Ghats of

- 1 India. *Pondy Papers in Ecology*, 10: 1-71, Available from <<http://hal.archives-ouvertes.fr/hal-00509952/fr/>>
- 2
- 3 Proisy, C., Mougin, E., Fromard, F., Trichon, V. & Karam, M. A. (2002). On the influence of  
4 canopy structure on the polarimetric radar response from mangrove forest.  
5 *International Journal of Remote Sensing*, Vol.23, No.20, pp.4197-4210, ISSN: 0143-1161
- 6 Proisy, C., Couteron, P. & Fromard, F. (2007). Predicting and mapping mangrove biomass  
7 from canopy grain analysis using Fourier-based textural ordination of IKONOS  
8 images. *Remote Sensing of Environment*, Vol.109, No.3, (August 2007), pp.379-392,  
9 ISSN: 0034-4257
- 10 Rao, A. R. & Lohse, G. L. (1996). Towards a texture naming system: Identifying relevant  
11 dimensions of texture. *Vision Research*, Vol.36, No.11, (June 1996), pp.1649-1669,  
12 ISSN: 0042-6989
- 13 Rich, R. L., Frelich, L., Reich, P. B. & Bauer, M. E. (2010). Detecting wind disturbance  
14 severity and canopy heterogeneity in boreal forest by coupling high-spatial  
15 resolution satellite imagery and field data. *Remote Sensing of Environment*, Vol.114,  
16 No.2, (February 2010), pp.299-308, ISSN: 0034-4257
- 17 Richards, P. W. (August 1996). *The Tropical Rain Forest. An Ecological Study*, 2nd edition,  
18 Cambridge University Press, ISBN: 9780521421942, Cambridge
- 19 Vincent, G. & Harja, D. (2008). Exploring Ecological Significance of Tree Crown Plasticity  
20 through Three-dimensional Modelling. *Annals of Botany*, Vol.101, No.8, (May 2008),  
21 pp.1221-1231, ISSN: 1095-8290
- 22 Zhao, K., S. Popescu and R. Nelson (2009). Lidar remote sensing of forest biomass: A scale-  
23 invariant estimation approach using airborne lasers. *Remote Sensing of*  
24 *Environment*, Vol( 113), No.1, (January 2009), pp. 182-196, ISSN: 0034-4257